

High-temperature and low-stress creep anisotropy of single-crystal superalloys

L. Agudo Jácome^{a,*}, P. Nörtershäuser^a, J.-K. Heyer^a, A. Lahni^a, J. Frenzel^a, A. Dlouhy^b,
C. Somsen^a, G. Eggeler^a

^a *Institut für Werkstoffe, Ruhr-Universität Bochum, 44780 Bochum, Germany*

^b *Institute of Physics of Materials, Academy of Sciences of the Czech Republic, Žitkova 22, 616 62 Brno, Czech Republic*

Received 29 October 2012; received in revised form 24 January 2013; accepted 26 January 2013

Available online 1 March 2013

Abstract

The high-temperature and low-stress creep (1293 K, 160 MPa) of the single-crystal Ni-based superalloy LEK 94 is investigated, comparing the tensile creep behavior of miniature creep specimens in [001] and [110] directions. In the early stages of creep, the [001]-direction loading shows higher minimum creep rates, because a greater number of microscopic crystallographic slip systems are activated, the dislocation networks at γ/γ' interfaces accommodate lattice misfit better, and γ channels are wider. After the creep rate minimum, creep rates increase more strongly as a function of strain for [110] tensile loading. This may be related to the nature of rafting during [110] tensile creep, which results in a more open topology of the γ channels. It may also be related to more frequent γ' cutting events compared with [100] tensile creep.

© 2013 Acta Materialia Inc. Published by Elsevier Ltd. All rights reserved.

Keywords: Superalloy single crystals; Creep anisotropy; Rafting; Dislocations; Deformation mechanisms

1. Introduction

Creep [1–10] represents an important part of the load spectrum of single-crystal Ni-based superalloys (SX), which are used for first stage blades of gas turbines, where they operate close to their melting points [3,11–16]. The present study investigates LEK 94 superalloy single crystals [17]. The microstructures of SX exhibit large- and small-scale heterogeneities. The large-scale heterogeneities are associated with the evolution of the material's microstructure during solidification [15,16]. The spacing between primary dendrites in the dendrite microstructure can be of the order of 250 μm . The fine-scale heterogeneities are associated with the γ/γ' microstructure, which consists of cuboidal precipitates of the γ' phase (with an

average cube edge length of 0.4 μm), filling up to 70% of the volume. The γ' precipitates are separated by thin γ channels (~ 30 vol.%, with an average channel width of 70 nm). The γ phase has a face-centered cubic (fcc) crystal structure, while the γ' phase is an ordered $L1_2$ structure. It is well known that alloy elements partition during solidification, and that the chemical compositions between the centers of dendrites and the former interdendritic regions differ [16]. This holds equally for the smaller scale, where preferential partitioning of different elements in γ' cubes and γ channels is observed [18,19]. Fig. 1 shows a montage of scanning electron microscopy (SEM) micrographs, which were taken from a material after a short [001] tensile creep exposure (9 h at 1293 K and 160 MPa). The montage extends from a cast micro pore (in a former interdendritic region; top of Fig. 1) towards the center of a dendrite (bottom of Fig. 1). Micrographs at higher magnifications from three typical locations (top, close to the pore in the interdendritic region; middle, in the transient region between dendritic

* Corresponding author. Present address: Bundesanstalt für Materialforschung und -prüfung, Unter den Eichen 87, 12205 Berlin, Germany. Tel.: +49 30 8104 4032; fax: +49 30 8104 1517.

E-mail address: leonardo.agudo@bam.de (L. Agudo Jácome).

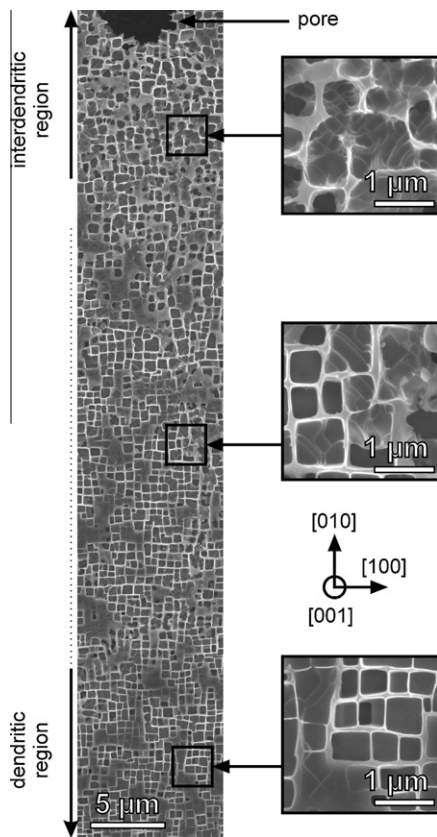


Fig. 1. Montage of SEM micrographs taken from a material that was exposed to creep at 1293 K and 160 MPa for 9 h ([001] tensile creep): (top) cast pore in a prior interdendritic region; (bottom) center of a dendrite. SEM images from three locations were taken at higher magnifications (shown next to montage). Material state 2 from Table 1.

and interdendritic region; bottom, close to the dendrite center) are shown next to the montage.

Creep of single-crystal superalloys has been studied extensively. A number of elementary dislocation mechanisms have been identified, including the filling of γ channels with dislocations [20–23], the formation of dislocation networks around γ' particles [23–25] and the pairwise cutting of the γ' phase by two γ channel dislocations [26–32]. Rafting, the directional coarsening of the γ' phase perpendicular to the direction of the applied load (for a negative misfit alloy loaded in $\langle 100 \rangle$ direction), is a well-known microstructural instability [33–37]. Some of these elementary deformation and coarsening processes have also been reported for the alloy investigated in the present study [31,38,39]. For the objectives of the present work, it is important to highlight that a full set of short-term creep data from the temperature regime >1273 K has been published [39]. Tensile creep data for $\langle 001 \rangle$, $\langle 110 \rangle$ and $\langle 111 \rangle$ directions were reported, and the stress and temperature dependences of the secondary creep rate were documented [39]. When comparing the [001] and the [110] creep data published by Mälzer and co-workers [39], two observations after creep at 1293 K and 160 MPa merit attention. First, the [110] tests yielded lower mini-

um creep rates than the $\langle 100 \rangle$ experiments. Second, it was found that the increase in the creep rate with strain was more pronounced for [110] than for [001] experiments. This interesting finding has not yet been explained in the literature. The [110] direction is generally considered as being weaker than the [001] direction (e.g., Refs. [40–43], even though the results from Mälzer and co-workers [39] suggest the opposite for the early stages of creep. The data of Mälzer et al. [39] are supported by other results [44–46], which, however, have not received much attention. Therefore, one objective of the present work is to provide additional mechanical evidence on the anisotropy in the early creep stages. It also has to be established why the increase in creep rate after the creep rate minimum so strongly depends on crystallography. There is a need to perform SEM and transmission electron microscopy (TEM) investigations of the γ/γ' morphology and of the dislocation structures in specimens that were interrupted early in creep life, like the material shown in Fig. 1. Unfortunately, such material states have so far only received limited attention. The main objective of the present work is to re-examine the mechanical data published by Mälzer et al. [39] and to provide a microstructural explanation for the differences in the early stages of [001] and [110] tensile creep tests in single-crystal Ni-based superalloys.

2. Experiments

2.1. Material and miniature creep specimens

The material investigated in the present work is the single-crystalline superalloy LEK 94. Details on chemical composition and heat treatment of this alloy have been reported elsewhere [39]. The role of cast micropores in creep rupture was revealed by Mälzer et al. [39]. Dislocation cutting processes were observed in the specimen after creep rupture, where two channel dislocations with different Burgers vectors b jointly shear the γ' phase [31,38]. So far no microscopic assessment of specimens was performed on material that was crept to low accumulated strains. In the present work, a miniature creep specimen test technique has been employed [47–49]. The miniature creep specimens are machined by an iterative procedure involving orienting the material in a Laue camera and subsequent spark erosion machining [39,48]. The tensile specimens are precisely aligned, and have an orientation error $<2^\circ$.

2.2. Creep testing

Interrupted creep tests were performed at a temperature of 1293 K and a stress of 160 MPa. Fig. 2a and b presents creep data from four tests, two of which were interrupted after 0.1% and two after 0.4% strain. Fig. 2a shows the strain ϵ vs. time t tensile creep data for the two loading directions [001] and [110]. Fig. 2b shows a log–linear plot of strain rate $\dot{\epsilon}$ vs. strain ϵ . As shown in Fig. 2a and b, the

Download English Version:

<https://daneshyari.com/en/article/10620281>

Download Persian Version:

<https://daneshyari.com/article/10620281>

[Daneshyari.com](https://daneshyari.com)